Chinese Chemical Letters 34 (2023) 107198

Contents lists available at ScienceDirect

Chinese Chemical Letters

journal homepage: www.elsevier.com/locate/cclet

Halogen-based functionalized chemistry engineering for high-performance supercapacitors

Wuquan Ye[a,1], Hongfei Wang[a,1], Junling Shen[a], Shahid Khan[a], Yijun Zhong[a], Jiqiang Ning[b], Yong Hu[a,c,*]

[a] Key Laboratory of the Ministry of Education for Advanced Catalysis Materials, Department of Chemistry, Zhejiang Normal University, Jinhua 321004, China
[b] Department of Optical Science and Engineering, Fudan University, Shanghai 200438, China
[c] Hangzhou Institute of Advanced Studies, Zhejiang Normal University, Hangzhou 311231, China

ARTICLE INFO

Article history:
Received 16 December 2021
Revised 6 January 2022
Accepted 1 February 2022
Available online 6 February 2022

Keywords:
Halogen-based functionalized chemistry
Doping strategy
Decoration strategy
Electrode materials
Supercapacitors

ABSTRACT

Supercapacitors (SCs) are rated as the foremost efficient devices bridging the production and consumption of renewable energy. To address the ever-increasing energy requirements, it is indispensable to further develop high-performance SCs with merits of high energy-density, acceptable price and long-term stability. This review highlights the recent advances on halogen-based functionalized chemistry engineering in the state-of-the-art electrode system for high-performance SCs, primarily referring to the doping and decoration strategies of F, Cl, Br and I elements. Due to the discrepancy of electronegativity and atomic radius, the functionalization of each halogen element endows the substrate materials with different physicochemical properties, including energy bandgap structure, porosity distribution and surface affinity. The principle of halogen embedment into host materials by precisely controlling ionic adsorption and electronic structure is presented. And, the vital perspectives on the future challenges of halogen functionalization are also discussed. This work aims to deepen the understanding of halogen-based functionalized strategies to motivate further research for the development of high-performance SCs, and it also provides a prospect for exploring new material modification methods for electrochemical energy storage.

1. Introduction

The continuous improvement of living standards enhanced the demand for electronic power products, such as electric vehicles, mobile electronic equipment, intelligent nursing electronic sensors [1–6]. Meanwhile, the greenhouse effect caused by the massive combustion of fossil fuels has also been the focus of the world. It is expected that renewable energy will replace non-renewable energy in the immediate future, and this trend has triggered the birth and fast exploitation of recent energy vehicle manufacturers. Unfortunately, the stability problem and battery insecurity hinder the market competitiveness of today's new electrical products. To solve the growing requirements of electricity and ecologically friendly exploitation of human society, researchers are committed to integrating traditional capacitors into batteries to achieve high power/energy density. Thereinto, supercapacitors (SCs) are endued with the important task for meeting the urgent needs of energy storage applications.

SCs are a late-model type of energy storage devices between traditional capacitors and chemical power supply devices, also known as double layer capacitors and electrochemical capacitors. And principally, it can also be divided into electrical double layer capacitors (EDLCs) and faradic pseudo capacitors (PCs) based on energy storage mechanism, where the charge transfer mostly occurs at the surface of bulk electrode active materials. Compared with traditional capacitors, SCs not only exhibit large specific capacitance, but also inherit the merits of fast charging rate, long-period service duration, extraordinary temperature adaptability, green energy saving and sustainable environmental benignity. Furthermore, SCs are able to deliver high power density that can afford large currents in a short time, which is unattainable for chemical power supply devices. This unparalleled property is well matched to the instantaneous large current requirements for some electrical equipment [7–11]. As a comparison, the performance parameters of SCs, traditional capacitors and batteries are demon-

* Corresponding author.
E-mail address: yonghu@zjnu.edu.cn (Y. Hu).
[1] These authors contributed equally to this work.

https://doi.org/10.1016/j.cclet.2022.02.004
1001-8417/

Table 1
Basic electrochemical parameters of traditional capacitor, supercapacitor and battery.

Parameters	Supercapacitor	Traditional capacitor	Battery
Charging time (s)	1~30	10^{-6}~10^{-3}	103~104
Energy density (Wh/kg)	1~10	<0.1	50~200
Power density (W/kg)	1000~2000	>10,000	50~200
Cycle efficiency	90%~95%	100%	70%~85%
Cycle life (s)	>100,000	infinite	500~2000

strated in Table 1. In view of their excellent electrochemical performances, SCs are diffusely employed in consumer electronics, intelligent grid systems, new energy technologies, industrial energy-saving networks, solar generation projects, pulse power devices, *etc.* [12–17]. However, the relatively limited energy density (1–10 Wh/kg) of SCs makes them incompetent for practical heavy-duty equipment and long-period operation. Based on the calculation formula ($E=(1/2)\times C\times V^2$), the energy density can be improved by increasing the specific capacitance and broadening the cell voltage. Electrodes and electrolytes (as two indispensable components of SCs) are the starting point for further optimization of electrochemical performance. Therefore, the development of advanced electrode and electrolyte materials has become the formidable challenges of energy storage for researches [18–23]. As lately perceived, the research emphasis is primarily placed on the enlargement of specific surface areas, regulation of pore size distribution, construction of special nanostructure, modification of surface functional groups in electrodes as well as the designing of suitable electrolyte system to afford high potential.

Surface functionalization, especially chemically substituted or decorated strategy, has been considered as one of the most available methods to promote the specific capacitance [24–27]. Numerous previous studies have been taken to assess the contribution of heteroatom doping, especially when incorporated into electrode materials, mainly including nitrogen, boron, sulfur and phosphorus *etc.* [28–32]. In all cases, doping-induced charge redistribution may initiate a great deal of random structural defects and irregular lattice arrangement through theoretical calculations and experimental results [30]. Therefore, we prefer to get some summarized progress of doping strategies for the guidance of future work. Currently, the researches on nitrogen and sulfur functionalized electrode materials are relatively more mature [33,34], thus interrelated reviews have also been reported extensively to describe the samples preparation process and electrochemical measurement performance [35]. Nonetheless, there are few overviews of functionalized chemistry based on the whole halogen family for SCs in detail. This sort of functionalized strategies always pays close attention to the bonding relationship (covalent and ionic bond) as well as the relevant microstructure modification. Typically, halogen atoms with high electronegativity have been assumed to boost efficient electron transfer. Besides, the halogen-based functionalized electrode materials can improve electrical/electronic conductivity and provide abundant faradic electrochemical active sites, offering attractive potential for facilitating the development of SCs (Fig. 1). A mass of reviews about the halogen-based strategies in rechargeable ion batteries have been reported over the past few years, but the overall organization of relative work in SCs has been rarely addressed [36]. Inspired from the aforementioned literatures, the impact of halogen functionalized chemistry on the state-of-the-art SCs in recent years will be comprehensively summarized, specifically highlighting various types of halogen-based doping strategies (F, Cl, Br and I) in electrodes. Thereafter, the corresponding internal relationship between performance enhancement and action mechanism is thoroughly discussed. Furthermore, the principle of halogen embedment into host materials by precisely controlling ionic adsorption and electronic structure is also presented. Lastly, we wish to provide some guidance and future direction for the development of halogen-based chemistry in SCs.

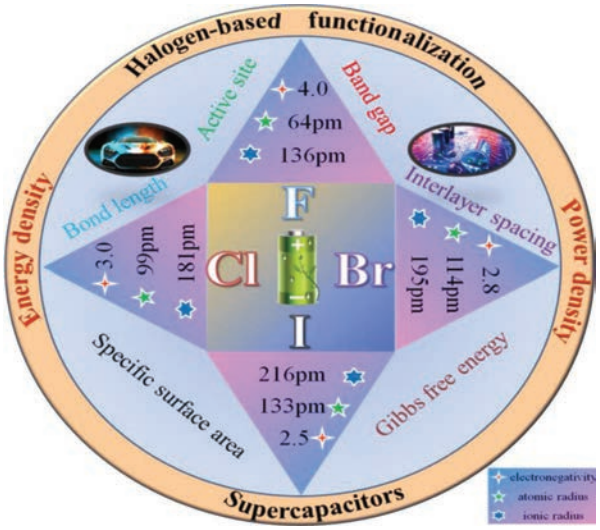

Fig. 1. Halogen-based functionalized chemistry for high-performance SCs.

2. Types of halogen-based functionalized chemistry

It should be noted that the chemical properties of halogens are very similar. They all have 7 electrons on the outermost electron shell, and are inclined to obtain one electron to form halide ions with a stable octagonal structure. With the molecular weight increasing, the dispersion force between halogen molecules gradually increases, and the color becomes darker. Their melting point, boiling point, density and atomic volume also increase in sequence. As the atomic radius increases, the ability to obtain electrons decreases, so F is the most oxidizing among four elements. In addition, higher electronegativity will induce the degree of polarization between halogen atoms and host atoms, enhancing the connection force between molecules [37]. Moreover, the larger atomic volume and mass will promote the increase of dipole moment and bond energy, resulting in the decrease of the bonding force [38]. Therefore, F and Cl are more widely used in the electrode surface functionalization.

Previously, Zhang *et al.* [39] reported that the introduction of oxygen vacancies into metal oxides can markedly regulate their intrinsic electronic properties and stimulate impure states, consequently improving the electrical conductivity of electrodes. The resultant oxygen-defective electrode exhibits substantially superior charge storage capability to pristine samples benefited from these advantages. Similar to the contribution of oxygen defects, engineering halogen species can also tune the donor density of host electrode materials, induce defective sites in its bandgap and boost the kinetics of surface redox reactions. For instance, the incorporation of assorted halogen heteroatoms into carbon-based materials will induce a positive doping, thus modulating the Fermi level and engineering the electronic properties [24,25]. Furthermore, the

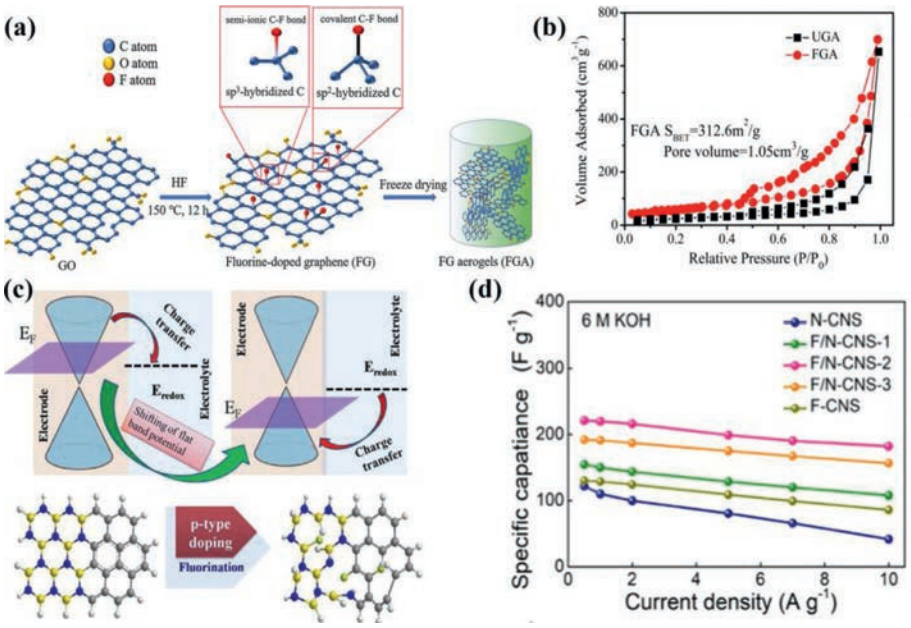

Fig. 2. (a) Scheme of the preparation of FGA. (b) N_2 adsorption-desorption plots of FGA and UGA. Reprinted with permission [41]. Copyright 2020, Springer. (c) Schematic illustration of the simulative atomic structure, band structure and charge transfer. Reprinted with permission [42]. Copyright 2018, Elsevier. (d) Specific capacitances of all electrodes at various current densities. Reprinted with permission [43]. Copyright 2020, American Chemical Society.

decoration of halogen atoms can probably alter the microstructure of carbon materials, resulting in surface wrinkles and inner pores. With the increasing of specific surface area (SSA), the modified carbon materials can enhance charge storage and possess higher specific capacitance and superior cycling stability for SCs [39]. To date, according to the elemental classification there are mainly four types of halogen-based functionalized strategies exist, such as F, Cl, Br and I. More attention should be paid to halogen functionalization chemistry for SCs due to the recent accomplishment in the comprehensive analysis and understanding of the effect of halogen atoms.

2.1. F-based functionalized chemistry

Among the halogen elements and even other non-metallic elements, F possesses the highest electronegativity (4.0) than the same family of elements (3.0 of Cl, 2.8 of Br and 2.5 of I) and other common non-metallic elements (3.5 of O, 3.0 of N, 2.5 of C and 2.0 of B). Based on this fact, the electron density is concentrated on polarized C-F, which endows the electrode materials with superior properties. Fluorine-doping (F-doping) and fluorination of carbon materials usually involve grafting fluorine atoms directly onto the carbon rather than into the carbon lattice [24]. Based on the electronegativity difference of 1.5 between carbon and fluorine, the C-F bonds derive from fluorinated carbon materials primarily exhibit three characters, such as ionic, semi-ionic and covalent bond. The content of each C-F bond can be precisely regulated by changing reaction time, temperature and choice of fluorination agents, essentially altering the physical and chemical properties of carbonaceous precursors. Concretely, DFT theoretical calculation confirms that covalent C-F bonds increase the strain in the 2D graphene structure and cause the formation of interlaminar C–C bonds disorder [40]. Indeed, Jin *et al.* [41] deployed a facile hydrothermal method to prepare a 3D F-doped graphene aerogel (FGA) with abundant semi-ionic C-F bonds applied in electrodes, which ensures higher electronic conductivity and more active sites (Fig. 2a). It can be found from the Brunauer-Emmett-Teller (BET) test that the SSA and total pore volume of the FGA are both higher than those of undoped graphene aerogel (UGA), indicating no evident of irreversible lamellar stacking exists after F-modification treatment (Fig. 2b). It's worth noting that F doping can also alter the superlattice to some extent. Sanjit *et al.* [42] carried out an F doping technology to minimize the band gap from ~2.1 eV to ~1.79 eV for the hybrid of the hexagonal boron nitride (h-BN) and reduced graphene oxide (rGO) (Fig. 2c). In this case, the h-BN/rGO superlattice behaves as an n-type semiconductor and F-doped superlattice acts as a p-type semiconductor, in which F is adsorbed at N sites. Benefiting from the contribution of the redox charge reaction, the F-doped h-BN/rGO delivers a specific capacitance of 1250 F/g at 10 mV/s, which is 130% larger than that of the non-doped material. In addition, the asymmetric SC presents a desired relaxation time constant (~0.39 ms), which can guarantee the implementation of high-efficiency power delivery and tremendous charge-discharge capacity.

It is well known that various electrode materials still suffer from sluggish ion-transfer kinetics. Thereinto, Zhu *et al.* [43] reported a molten-salt pyrolysis strategy to synthesize an F, N co-doped porous carbon nanosheet (F/N–CNS), which exhibits rapid kinetics and enhanced pseudocapacitive features. The molten salt strategy as a facile and confined process can not only supply a desirable reaction medium to obtain ultrathin carbon architectures, but also inhibit the liberation of N- and F-containing groups. As shown in Fig. 2d, the F/N–CNS-2 renders superior specific capacitance and better rate performance than that of solitary N doped samples. Zhao *et al.* [44] applied the ZIF-67 as a typical template *via* calcination and hydrothermal processes to synthesize N, F dual-doped hierarchical nanoporous carbon polyhedron (NFHPC) with a high degree of graphitization as the negative electrode, which possesses a remarkable specific capacitance value of 305 F/g at the current density of 1 A/g (Fig. 3a). Noteworthy, the NFHPC exhibits superior electrochemical performance than other N, P doped carbon materials. This also confirms that appropriate incorporation of F element is beneficial to decrease the equivalent series resistance and improve the specific capacitance value. Geng *et al.* [45] reported that the specific capacitance can be adjusted from the aspect of the BET surface area after fluorination. Additionally, relatively high electronegativity can also effectively regulate the band gap structure of carbon materials. The optimization of both mor-

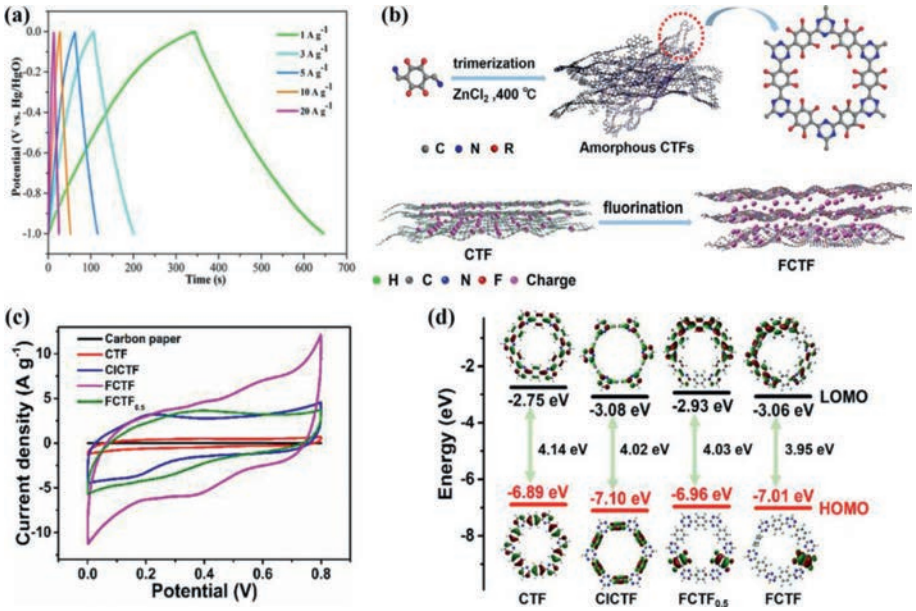

Fig. 3. (a) Galvanostatic charge-discharge (GCD) curves of NFHPC electrode. Reprinted with permission [44]. Copyright 2020, Elsevier. (b) The synthetic procedure of the CTFs and the schematic display of the interlayer distance evolution. (c) CV curves at 10 mV/s. (d) HOMO and LUMO levels. Reprinted with permission [52]. Copyright 2020, Elsevier.

phology and electronic structure can make up the shortcoming derived from the molar mass increase of halogen atoms and make the specific capacitance increase instead of decrease. However, in some cases, the fluorination would decrease the conductivity of carbon substrate, which can be ascribed to the C-F covalence bonds [46]. Besides, the regulation of semi-ionic characteristics for C-F bonding enables the improvement of conductivity [45,47-49]. Sun *et al.* [50] also reported that the presence of semi-ionic C-F bonding in fluorinated graphene can decrease the charge transfer resistance and improve the rate capability. An effective strategy is to fabricate the C–H···F hydrogen bonds for the transfer of electron clouds from C-F bonds to F atoms, leading to the transformation from covalent C-F bonds to semi-ionic C-F bonds.

Likewise, the interlayer spacing of some other 2D materials can also be regulated, which is conducive to the rapid storage of charges and provides a precious opportunity for structural modification. Triazine-based frameworks (CTFs) denote one kind of novel organic skeletons with plentiful atomic-scale pores assembled by organic molecules. Interestingly, the extended π-electronic conjugation and well-defined hierarchical nanostructure create accessible ion channels, which greatly shorten the mass transfer pathway and release many ions adsorption sites [51]. Nevertheless, the mediocre electron/ion conductivity and detrimental stacking effect of polymers seriously stem the application of CTFs as electrode materials in SCs. The interlayer control *via* rational grafting redox-active units into backbones is regarded as an ideal strategy to solve the issue of structural instability while halogens are desired potential candidates. As illustrated in Fig. 3b, Gao *et al.* [52] adopted a fluorine-substitution strategy to tailor the energy band structure in CTFs and facilitate the electron transportation process. Fig. 3c demonstrates that the fluorinated CTF (FCTF) exhibits the largest integrated cyclic voltammetric (CV) area as compared to other CTFs, implying the better electrochemical performance of FCTF. In essence, the theoretical calculation elucidates that the fluorine-functionalized CTF displays a lower energy gap than that of pristine material, which suggests a reduced internal resistance and improved charge transportation (Fig. 3d). Consequently, the FCTF shows the maximum specific capacitance of 379 F/g at the current density of 1 A/g, superior cyclic stability (96.8%) and Coulombic efficiency (99.6%) over 10,000 cycles. These results suggest that decorated F atoms are believed to own the function of enlarging the interlayer space and exposing sufficient active sites for faradic reactions, further widening the utilization of fluorine-functionalized strategy.

The F-based function chemistry applies not only to EDLC materials but also to pseudocapacitor materials. Zhang *et al.* [53] introduced halogen ions into β-FeOOH to change the Fe-O bond length and structural distortion, which reduced the bad gap and improved the electric conductivity. The negative electrode of β-FeOOH(F) delivers a high specific capacity of 391.9 F/g at 1 A/g with out-standing rate capacity and cycling stability. $Ti_3C_2T_x$ MXene (T = O, F, OH, *etc.*) is another type of promising electrode materials for SCs [54–58]. However, the re-stacking problem and excess terminal groups may restrict ions diffusion and degrade the electrochemical performance. The surface engineering based on F functional groups is deemed to be very essential in controlling the morphology and electronic structure of MXene materials. Chen *et al.* [57] carried out alkalization and post-annealing treatments to modify the amount of T_x surface functional group of $Ti_3C_2T_x$, facilitating the intercalation of electrolyte K^+ ions into MXene layers.

Thus, F is the most reactive among the four as-mentioned halogen elements in this literature. When F atoms are incorporated into carbon matrixes, the resultant strong C-F bonds are formed and the original C–C bond length increases from 1.57 Å to 1.58 Å. The strategy of F-based functionalized chemistry can also improve the electronic conductivity and ion-transfer kinetics of metal-based electrode materials, as well as minimize the band gap and decrease the equivalent series resistance, thus boosting the electrochemical performance.

2.2. Cl-based functionalized chemistry

Numerous researches dedicated to improving the gravimetric specific capacitance of electrode materials in SCs. However, the low mass loading of the electrode leads to small area specific capacitance. There is no doubt that this is detrimental to some area-required applications, such as miniature electronics and the hu-

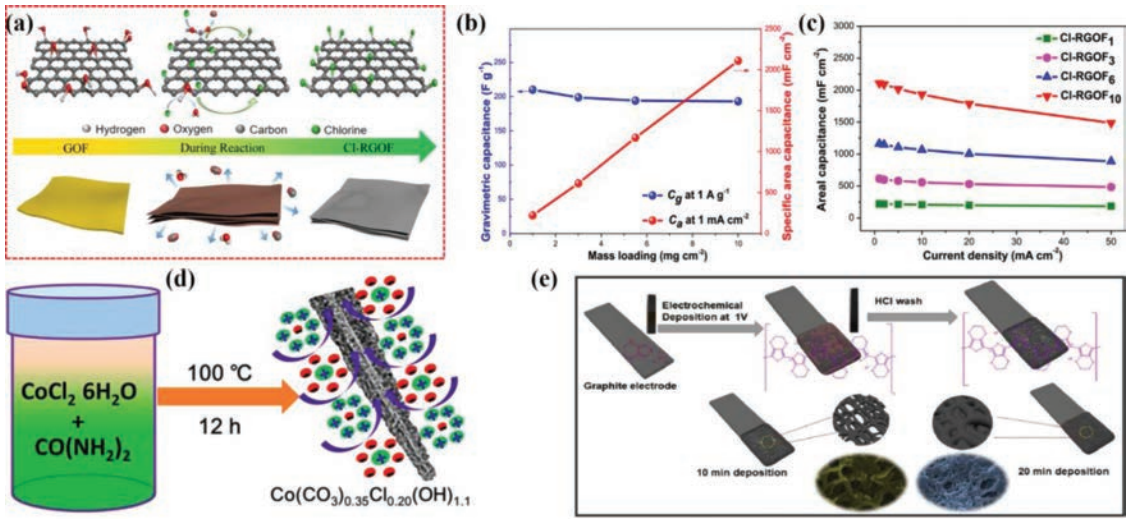

Fig. 4. (a) Schematic display of Cl-RGOF fabrication. (b) Variation of gravimetric (C_g) and areal capacitance (C_a) with the increasing of mass loadings. (c) C_a of all Cl-RGOF electrodes at different current densities. Reprinted with permission [67]. Copyright 2019, American Chemical Society. (d) Schematic illustration of hydrothermal preparation of $Co(CO_3)_{0.35}Cl_{0.20}(OH)_{1.10}$. Reprinted with permission [68]. Copyright 2015, Elsevier. (e) Scheme of Cl-doped PEDOT. Reprinted with permission [79]. Copyright 2020, Elsevier.

man body [59–63]. Increasing electrode thickness or mass loading is considered to be a valid approach to solve this problem. Sequentially, sluggish ion transfer kinetics following with severe internal resistance becomes an inevitable challenge, resulting in a sharp utilization decline of materials eventually [64–66]. Thus, precise synthesis of electrode materials is anticipated to be accomplished in terms of unique structure and composition, consequently producing more involved bulk active sites. The charged terminal anions acting as structural stabilizers can be applied to synergy with host molecules or ions, thereby promoting the deep diffusion of electrolytes and forming the favorable solvation molecules. In this regard, Cl-based functionalized strategy plays a significant role in this special structural modification.

To address the above ideology, Jiang *et al.* [67] proposed a facile HCl-treated solvothermal method to prepare Cl-doped rGO films (Cl-RGOFs) with outstanding areal electrochemical performance as shown in Fig. 4a. The electrical conductivity of Cl-RGOFs improved 2.5 times observably than that of RGOFs because of the electron-with-drawing effect caused *via* the doping of Cl. Furthermore, the areal capacitance of Cl-RGOF exhibits the linear enhancement with the mass loading (Fig. 4b). As a result, Cl-RGOFs with a mass loading value of 11 mg/cm^2 display an excellent areal capacitance of 2312 mF/cm^2 and remarkable capacitance retention property of 78.7% with increasing of current density from 1 mA/cm^2 to 20 mA/cm^2 (Fig. 4c). The assembled flexible SC presents strong capacitance holding at various mechanical bending states after repeating 500 times, which can be attributed to the result of successful Cl doping.

Transition metal oxides, hydroxides and their corresponding binary species can bring faradic redox reaction and achieve exceptional specific capacitance relative to carbon-based electrode materials, but they often suffer from the deteriorative intrinsic conductivity and cycling stability. Aiming at this aspect, Mahmood *et al.* [68] prepared a Cl-doped carbonated $Co(CO_3)_{0.35}Cl_{0.20}(OH)_{1.10}$ nanowires *via* a mild hydrothermal method (Fig. 4d). The engineered Cl doping technology endows the pristine layered material with specified interlayer spacing, well-defined porosity and hydrophilic nature for the deep permeation of electrolyte ions. Owing to the modified structure and advantageous Cl doping, the occurrence of deep faradic redox reaction in the inner active sites contributes to the extraordinary capacitance, rate capability and stability. Similarly, this strategy was also employed into the construction of all-in-one electrodes where the doped Cl components provide an accessible platform for the boosted transport of electrons from electrodes to current collectors. Zhao *et al.* [69] also synthesized chlorine-doped carbonated cobalt hydroxide nanowires *via* one-step hydrothermal method, and the electrode can reach more than 2150 F/g at 1 A/g, which is better than that of conventional electrodes.

Conducting polymers (CPs) are another type of expectant pseudocapacitive electrode materials that differ from metal oxides and carbon materials [70–72]. Poly(3,4-ethylenedioxythiophene) (PEDOT) is a commonly used conductive conjugated polymer that has been explored as SC electrode materials for its superior conductivity and narrow bandgap [73,74]. It is remarkable that the types of polymerization strategy can affect the electrical conductivity of PEDOT. The polymerization process demonstrates higher conductivity (300 S/m) than that of chemical vapor phase deposition (100 S/m) [75–78]. In addition, the redox reaction kinetics in the polymer matrix is also highly dependent on the surface heteroatom dopants. Up to now, $FeCl_3$ is often adopted as a dopant and oxidant for the chemical synthesis of Cl-doped PEDOT nanostructures. Rajesh *et al.* [79] proposed a straightforward electrochemical polymerization of Cl-doped PEDOT *in situ* on the graphite current collector for the first time (Fig. 4e). The optimal deposition and washing treatment create a distinct porous hierarchal Cl-PEDOT nanostructure without any extra additives. It is also possibly affirmed that the dead volume in the PEDOT matrix can be reduced obviously and the facilitated penetration of electrolyte ions is allowed after the Cl-based functionalized doping process. Therefore, the modified amorphous PEDOT is anticipated to be a potential SC electrode, since the final Cl-PEDOT delivers a superior specific capacitance of 480 F/g at 2 A/g and considerable cycling of ~95% after 10,000 cycles.

Cl atoms doping will enhance C–Cl bond length and lower the binding energy as compared to F. It also sheds light on that the stability of C–Cl bond is lower than that of C-F bond. For instance, it has been reported that Cl-doped graphene (1.1–1.7 nm) is visibly thicker than F-doped graphene due to the discrepancy of bond length. The Cl-based functionalized method can also improve the electronic conductivity. Specially, it is beneficial to the structural modification of materials, which can be employed in flexible SC. In addition, the optimized material is conducive to promoting electrolyte penetration.

2.3. Br-based functionalized chemistry

In some particular solvents, pristine materials limited by the polarity factor show low solubility and fail to disperse homogeneously. Generally, the increased dispersibility can be achieved by grafting compatible surface groups, making it possible for the subsequent processing of membranes, coatings and electrodes. In other words, functionalized surface chemistry can promote contact wettability by the required phase change, selective binding sites and stable doping components. Bromination is one of the most attractive routes to obtain highly reactive products for further reaction in spite of its common application in molecular intercalation or adsorption [80]. Br can be doped onto different matrixes by some proven techniques, such as direct exposure to Br_2 vapor, microwave or sonication assistant synthesis in liquid phase, photocatalytic addition using corresponding precursors and so on.

To date, graphene, as an indispensable carbon material, has been functionalized *via* covalent bonds, noncovalent bonds and ionic bonds. Covalent bonds can reveal the property of the introduced molecule. However, their formation conditions are strict [81]. Additionally, the physical properties of derivatives will diminish as sp^2 carbon framework converted to sp^3 hybridization [82–85]. Non-covalent interactions, such as π-π interactions, can maintain the integrity of sp^2 carbon framework. But the molecule dissociation often occurs easily owing to weak interactions [86]. With regard to ionic bond, it is robust in the mild conditions, but fragile in other hash environments including acid and base conditions [87]. As a result, it is necessary to exploit a novel functionalized solution for graphene and its derivatives that can improve their properties. Khan *et al.* [88] proposed a novel concept in the field of graphene functionalization with halogenated graphene. And the brominated graphene was functionalized with heteroatom-containing molecules to construct onium bonds. This strategy of forming onium bonds not only shows very strong interaction akin to covalent bonds, but also leaves over no byproducts through a facile process similar to the formation conditions of ionic bonds. Impressively, the XPS analysis unveils that brominated graphene predominantly forms onium bonds compared to chlorinated graphene and iodinated graphene, indicating a novel applicable field of Br-based functionalized chemistry. However, there are still two unavoidable disadvantages in graphene modification. One of them is the disordered distribution of functional groups, and the other is the existence of plenty of lattice defects. To address these problems, Hu *et al.* [89] adopted natural graphite functionalized with reductive covalent, as opposed to destructive GO-derived methodologies. Through the process of potassium reduction to graphite, negative charges can be distributed uniformly on graphene sheets. After that, they were subtly functionalized by the electrophile of molecular bromine. The molecular formula of graphene bromide derivative was abbreviated as C_{24}-Br (Fig. 5a), consistent well with the precursor of $C_{24}{}^{-}K^{+}$ graphite intercalation compounds. The graphene bromide product (denoted as C_{24}-Br-GBr) shows preeminent electrochemical performance than that of direct GO bromination due to the impeccable hexagonal lattice of graphene nanosheets. As demonstrated in Figs. 5b and c, the C_{24}-Br-GBr exhibits larger CV curves area and higher specific capacitance than that of Br_2-GOBr. In a word, the synergistic effect between Br functional groups and region-regularly nondestructive graphene lattices contributes significantly to the high performance of SC electrodes and guides a new direction for the future development.

In other respects, Br-based covalent bonds combined with the spatial stereo effect also play an outstanding role in the improved conductivity and stability for composite materials. Specifically, Br decorated conjugates show accelerated electron transfer and excellent electrolyte affinity. Zhang *et al.* [90] used a hydrothermal method to prepare subphthalocyanine/nickel molybdate (SubPc-Br/$NiMoO_4$) composite as electrode material. SubPc-Br was obtained from the reflux reaction of 1,2-dichlorobenzene and BBr_3 in the inert atmosphere of N_2. The crystal structure model presents a nearly triangular pyramidal shape, where its center is a B atom connected to a Br atom at the top of the cone. The stacking pattern of the SubPc-Br within an intramolecular dimer through the special form of "convex-convex, head-head" provides suitable sites and great contact areas for the successful location of $NiMoO_4$ particles. Eventually, the electrochemical experiments confirm that SubPc-Br can greatly boost the redox strength and mass transfer of $NiMoO_4$. As a matter of course, it delivers an impressive specific capacitance value of 1292 F/g. The cycling stability of SubPc-Br/$NiMoO_4$ can also be improved by 12.9% after 1000 cycles.

In summary, Br-based functionalized chemistry can promote contact wettability, conductivity, as well as dispersibility, which is also an effective solution to enhance the electrochemical performance. In most cases, Br atoms are inclined to physically absorb on carbon matrixes rather than interrupting the original sp^2 conjugated structure. The reports on the Br-based functionalized chemistry engineering are obviously less than that of F and Cl.

2.4. I-based functionalized chemistry

On account of the previous literature, foreign heteroatom functionalized modification primarily optimizes the conductivity and electrochemical performance by increasing the carrier density in host matrixes. As the last non-radioactive element in halogens, iodine not only possesses high electronegativity, but also demonstrates high earth abundance, and I-modification has aroused great investigation attention. Accordingly, the adoption of iodine can induce the involvement of triiodine ($I_3{}^{-}$) and pentaiodine ($I_5{}^{-}$) polyanions and enhance the charge density, thus promising to decrease the internal resistance [91]. Nevertheless, it should be noted that doping iodine involves complicated process owing to its intrinsic large radius, where some special means should be taken to obtain stable products.

For instance, Zhao *et al.* [92] carried out a simple I_2-steam functionalization strategy to prepare I-functionalized rGO deposited on oxidized carbon yarn (I-rGO/OCY). The I-based functionalization can effectively inhibit the self-stacking of rGO layers to fulfill high utilization, thereby bringing into exert the inherent physical and chemical properties of graphene. Thereinto, the final I-rGO/OCY composite delivers the apparent amelioration in both electrical conductivity and hydrophilicity. The assembled all-solid-state fibriform supercapacitors present impressive specific capacitance, good cycling performance, excellent mechanical flexibility and stability. Otherwise, it is worth mentioning that iodine can be introduced as the pore-making agent to fabricate ordered micropores in starch-derived carbon. Luo *et al.* [93] adopted iodine as pore-making agent for the first time to increase the specific surface area of carbon *via* straightforward solvent heating and high-temperature carbonization at 1000 °C. When the temperature reaches a certain value, iodine begins to sublimate to produce a substantial number of hierarchical micropores, and the residual iodine is incorporated into the crystal lattice of carbon frameworks. As a result, the as-obtained I-doped porous carbon delivers a superior specific capacitance of 1216 F/g at 2 A/g and an energy density of 65.4 Wh/kg at a power density of 787.3 W/kg. Beyond this, I-doped strategy is also conductive for maintaining film structure and morphology in the process of carbonization of enzymatically synthesized amyloses (ESAs) polysaccharides [94].

Due to the fast development of wearable electronic devices, the devices that can take quick response to external stimulus have attracted extensively attention nowadays. In particular, there is an urgent need to develop some multi-functional integrated equip-

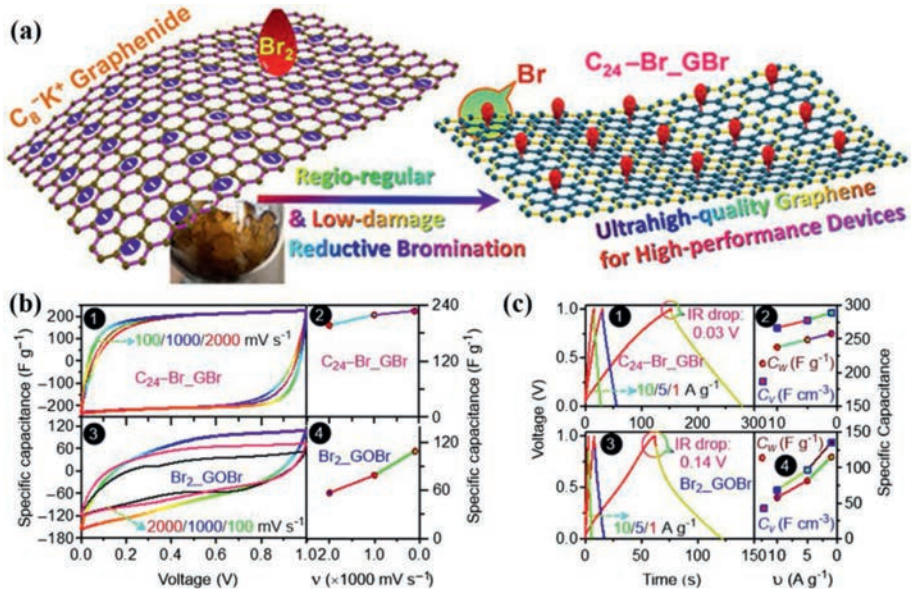

Fig. 5. (a) Schematic representation for the synthesis of brominated graphene. (b) CV curves as well as plots of the relation between specific capacitances and scan rates. (c) GCD curves as well as plots of the relation between specific capacitances and current densities. Reprinted with permission [89]. Copyright 2020, Chinese Chemical Society.

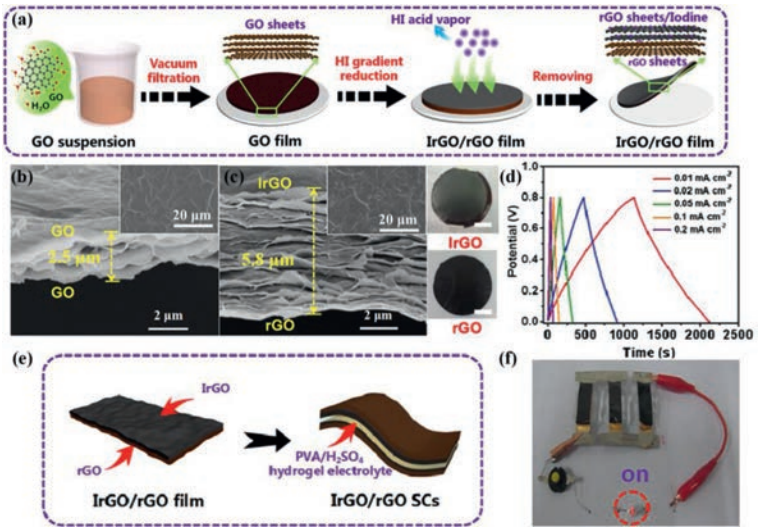

Fig. 6. (a) Preparation procedure of IrGO/rGO film. (b) Cross-sectional SEM image of GO film. (c) Cross-sectional SEM image of IrGO/rGO film. (d) GCD curves of IrGO/rGO film electrode at various current densities. (e) Schematic display of IrGO/rGO film used in the SC electrodes. (f) Digital photographs of SCs devices to illumine a LED. Reprinted with permission [95]. Copyright 2018, Elsevier.

ment, which puts forward requirements for volume minimization. In view of this issue, Yang *et al.* [95] successfully prepared I-doped rGO/rGO (I-rGO/rGO) with the merits of multi-responsive actuation and excellent capacitance as demonstrated in Fig. 6a. Through the regulation of HI treatment, the corresponding thickness of GO film was increased from 2.5 μm to 5.8 μm (Figs. 6b and c). However, while acted as multiple-responsive actuator materials, the single Janus film presents extraordinary static deformation, rapid mechanical bending rate of 70° per second as well as considerable repeatability. Conversely, when served as electrode materials, I-rGO/rGO based SCs show a high areal capacitance of 12.4 mF/cm^2 at 0.01 mA/cm^2 and a largest energy density of 1.09 μWh/cm^2 at 3.99 μW/cm^2 (Fig. 6d). Therefore, this advanced film can be employed as the core material for multifunctional SC (Fig. 6e). As a demonstration of application, the assembled SCs can light up a light-emitting diode (Fig. 6f). Based on these extraordinary advantages, this I-doped integrated material exhibits outstanding multiple response performances, which is potential in artificial intelligence fields. Like other halogen-based functionalized chemistry, I-based functionalized chemistry also shows excellent performance on pseudocapacitive materials. Wu *et al.* [96] prepared a series of bismuth-rich oxyiodides by hydrothermal route. The BiOI, $Bi_4O_5I_2$, Bi_5O_7I, and $Bi_7O_9I_3$ could be prepared by adjusting simply the pH values and OH^- concentrations. As a result, the $Bi_7O_9I_3$ shows the highest specific capacitance of 347 F/g.

To conclude, the I-based functionalized chemistry can boost the electronic conductivity, hydrophilicity and maintain the structure and morphology. In addition, it can inhibit the self-stacking and decrease the internal resistance. There are very few experimental and theoretical reports concerning I doping, which is due to the thermodynamic instability deriving from their lower electronegativity and larger radius.

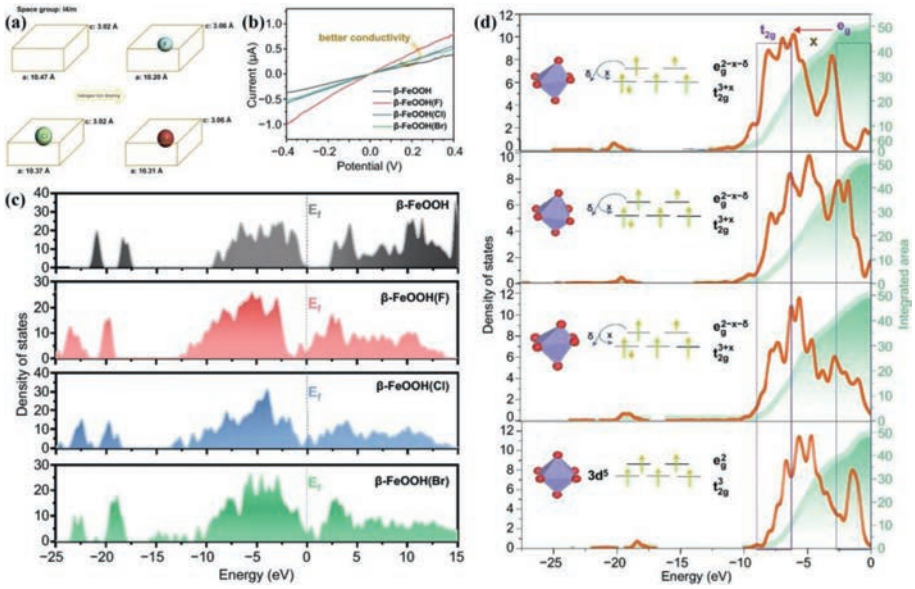

Fig. 7. (a) Schematic illustration of the contraction of β-FeOOH cell after doping halogen ions. (b) *I-V*, (c) DOS curves, (d) PDOS of Fe 3d valance band orbitals. Reprinted with permission [53]. Copyright 2020, Springer.

3. Principle of halogen-based functionalization

Although the excellent energy storage capacity of halogen-based functionalized strategy on SCs has been proven, so far, the idea of material design still mainly relies on routine trial-and-error methods. For EDLCs, the first-principles calculations have been done to elaborate the energy storage mechanism and charge storage capability of halogen doping. To rationally design metal-free carbon-based electrode materials, Gao *et al.* [97] employed DFT methods to calculate Gibbs free energy of H^+ adsorption (ΔG_{H^*}) for all the possible halogen-doping active structures. ΔG_{H^*} can be used as the descriptor to predict the capacitance variation trend with different dopants involvement. In short, the active sites for energy storage are identified in the range of $0 < \Delta G_{H^*} < U_d$. The upper bound U_d is the decomposition voltage of aqueous electrolytes (1.23 V), and the lower bound is $\Delta G_{H^*} = 0$. Those outside the above range are inactive sites. Furthermore, the maximum energy density can be also screened successfully by the intrinsic descriptor. Such prediction is in good agreement with the experimental results. This descriptor offers a reference direction for designing the desired carbon-based electrode materials.

For pseudocapacitive electrode materials, the charge storage will take the form of chemisorption instead of physical adsorption. The embedment of halogen ions contributes to coordinating the electronic structure of host materials. Based on the incorporation of F^-, Cl^- and Br^-, β-FeOOH as the model material was investigated by theoretical calculations coupled with experiments [53]. Owing to the strong reducing ability of I^-, it is difficult to obtain stable β-FeOOH(I) phase. The smaller anion radius and lower energy make it possible for halogen ions to spontaneously insert into β-FeOOH open-framework structure. According to the premise of geometry optimization, some important microstructure parameters (such as bond angle, bond length and electric charge density) were successfully tuned. Moreover, high electronegativity will also induce the electrostatic interaction between X^- (X = F, Cl, and Br) and β-FeOOH, thereby reducing the distance between Fe^{3+} and X^- as well as leading to slight contraction of unit cell size. As for the electrical conductivity, the hybridization between X^- 2p orbitals and Fe 3d orbitals will increase the electron density in the valence band and reduce the band gap. Intuitively, the valence band curve of β-FeOOH(X) is closer to the Fermi level than that of pristine β-FeOOH in the total density of states (DOS) curves (Fig. 7). Among them, the regulation of F ions takes the best effect to enhance the charge carrier excitation and promote the migration to conduction band. Similarly, the principle of minimum energy results in the change of electronic configuration for Fe 3d orbitals from $t_{2g}^3e_g^2$ to $t_{2g}^{3+x}e_g^{2-x-\delta}$ (Jahn-Teller effect). As a result, the charge-transfer energy drops from 7.52 eV for β-FeOOH to 6.76 eV, 7.37 eV and 7.04 eV for β-FeOOH(F), β-FeOOH(Cl) and β-FeOOH(Br), respectively. In addition to the lattice structural distortion and electronic structure adjustment, impressively, the wettability of host materials can also be affected by halogen embedment. In 1 mol/L Na_2SO_3 electrolyte, the contact angle of electrodes was reduced from 74.2° for β-FeOOH to 46.0° for β-FeOOH(F), 54.2° for β-FeOOH(Cl) and 53.2° for β-FeOOH(Br), respectively (Fig. 8). These results can be explained by the adsorption energy of SO_3^{2-}. β-FeOOH(F) exhibits the lowest adsorption energy among all samples, which is favorable to triggering the redox reaction and achieving efficient energy conversion. The improvement of wettability also plays a significant role in enhancing the long cycle stability, obtaining over 80% of capacitance retention at a high current density of 10 A/g. Besides, the insertion of X^- will also cause the increase of metal ions valence state, that is, Fe element presents $3+\delta$. According to the Mulliken charge data and XPS measurements, the influence of F on the valence state of metals is greater than that of Cl and Br. In brief, the modification of electronic structure and ionic adsorption after halogen-based functionalization make the metal pseudocapacitive materials present superior SC performances.

4. Application of halogen-based functionalized chemistry on other fields

As an efficient optimization means for electrode materials, halogen-based functionalized chemistry has been proven in other energy storage fields, like Zn-ion and Li-ion batteries and electrocatalysis. In general, highly electronegative halogen atoms can act as electron donor sites while interacting with other metallic elements (alkali and alkaline earth metals). Meanwhile, surface decoration, like halogenation and halogen-enhanced chemical adsorp-

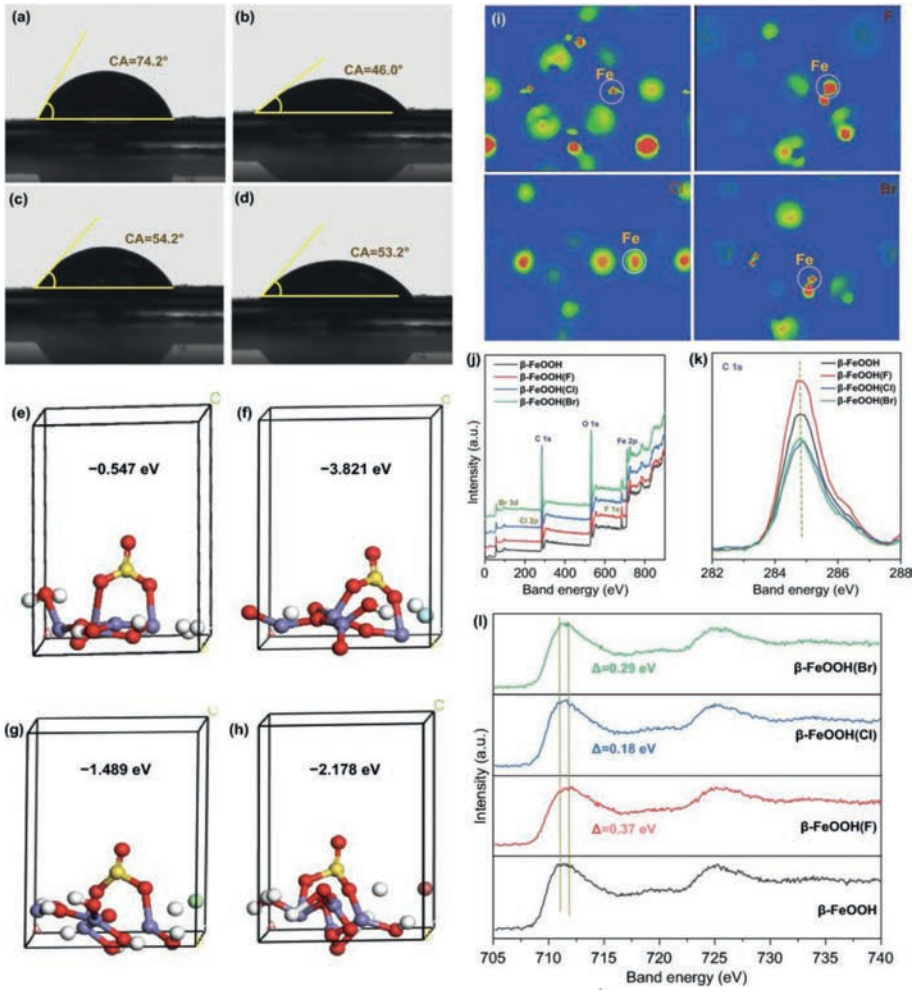

Fig. 8. (a-d) Contact angles and (e-h) adsorption energies for SO_3^{2-}. (i) Charge density differential diagram, and (j-l) XPS of β-FeOOH and β-FeOOH(X)s. Reprinted with permission [53]. Copyright 2020, Springer.

tion, is usually performed to keep the metallic electrode phase and improve the electrode/electrolyte interface [98].

For Zn-ion battery, the imperfections of irreversible phase transformation, volume expansion and structure collapse are inevitable for the cathode, which result in deteriorate capacity and poor cyclic stability [99–103]. To address these problems, Li *et al.* [104] developed a moderate F doping strategy to enhance the long-period cyclic stability of nickel cobalt carbonate hydroxide (NiCo-CH) cathode (Fig. 9a). It ought to be mentioned that the ionic radii of F and O ions are similar, which makes F own the ability to partially substitute the lattice oxygen species in metal oxides. Metal-F bonds with stronger ionic nature and lower polarization can result in a stable phase structure, higher lattice energy and stronger electrical conductivity of NiCo-CH. As shown in Fig. 9b, the NiCo-CH-F thus delivers an acceptable capacity of 245 mAh/g and superior rate performance, which should be ascribed to its superior charge and ions transfer kinetics (Fig. 9c). Furthermore, the *quasi*-solid-state battery ultimately keeps 90% after 7200 cycles and satisfying flexibility.

Qiu *et al.* [105] demonstrated that an appropriate amount of F substitution would take a prominent effect on the lattice structure of original $LiNi_{0.9}Co_{0.05}Mn_{0.05}O_2$ (NCM955). *In-situ* synchrotron radiation XRD reveals that the F substitution is crucial to suppress the irreversible phase transition and alleviate the interior stress deriving from the volume variation of unit cells, suggesting the reinforced structure and Li ions transport of NCM955-F1 (Fig. 9d). The resulted NCM955-F1 electrode can exhibit a maximum specific capacity of 194.4 mAh/g at 0.1 C, and it can still maintain 165.2 mAh/g at 5 C (Fig. 9e). Meanwhile, the capacity retention can keep 95.5% over 100 cycles at 2 C (Fig. 9f). Both superior rate performance and cycling stability are ascribed to the excellent structural stability of NCM955 deriving from the stronger Li-F bonds.

5. Summary and perspective

Halogen elements (Group 17 elements) with abundant material resources are well known for higher reactivity compared to Group 13–16 elements. We have summarized the recent advances and challenges towards halogen-based functionalized chemistry for SCs, containing F, Cl, Br and I. For each strategy, the synthetic method and refined corresponding characterizations with an in-depth understanding of the working mechanism for the ameliorative electrochemical performance are explicitly demonstrated in Table 2. To deal with the intrinsic issues of low conductivity, inaccessible wettability and instability of the electrode/electrolyte interface, the nanostructured electrode engineering through halogen-based surface doping and substitution is applicable. It is worth noting that halogen modification will change the wettability and make it more hydrophilic, which is conducive to the contact between electrodes and electrolytes. The improved hydrophilicity promotes the penetration of electrolytes and eventually leads to the stability of cyclic life, as listed in Table 3 [106–108]. In principle, the electronic and

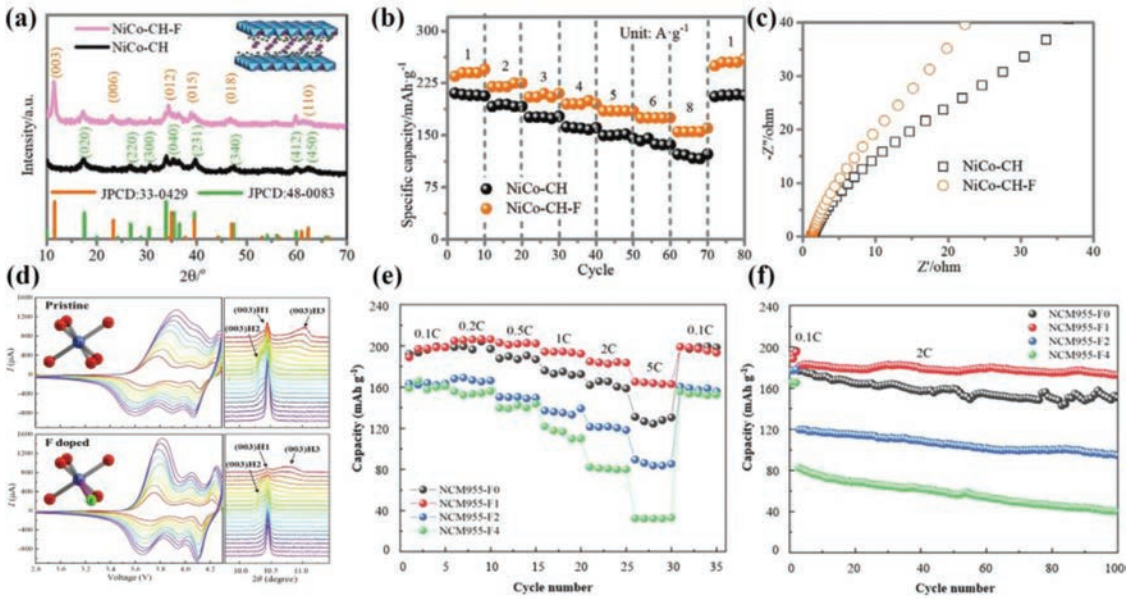

Fig. 9. (a) XRD patterns, (b) rate performance, and (c) Nyquist plots of NiCo-CH-F and NiCo-CH. Reprinted with permission [104]. Copyright 2020, Elsevier. (d) CV curves and corresponding *in-situ* XRD patterns, (e) rate capability, and (f) long-cycling performance of NCM955-F0 and NCM955-F1. Reprinted with permission [105]. Copyright 2021, Elsevier.

Table 2
Electrochemical performance of different halogen-based functionalized strategies on electrode materials.

Electrode materials	Agent	Electrolyte	Voltage window (V)	Specific capacitance	Rate capability	Cycle life	Energy density, power density	Ref.
FGA	40% HF	6 mol/L KOH	−1~0	279.8 F/g at 0.5 A/g	91% (10 A/g)	94% (5000 cycles)	26.2 Wh/kg, 899 W/kg	[41]
h-BN/ rGO	Ammonium fluoride	6 mol/L KOH	−1~0.5	1250 F/g at 10 mV/s	59% (200 mV/s)	77% (10,000 cycles)	87.5 Wh/kg, 6300 W/kg	[42]
F/N-CNS	PVDF	1 mol/L H_2SO_4	0~1	255 F/cm^3 at 1 A/g	82% (10 A/g)	100% (20,000 cycles)	18.8 Wh/L, 192 W/L	[43]
NFHPC	NH_4F/HF	3 mol/L KOH	−1~0	305 F/g at 1 A/g	77% (20 A/g)	95% (5000 cycles)	55.1 Wh/kg, 799.8 W/kg	[44]
CTFs	Tetrafluoro terephthalonitrile	1 mol/L H_2SO_4	0~0.8	379 F/g at 1 A/g	69% (10 A/g)	97% (10,000 cycles)	46.3 Wh/kg, 975 W/kg	[52]
Cl-RGOFs	HCl	6 mol/L KOH	0~1	210 F/g at 1 A/g	71% (100 A/g)	94% (5000 cycles)	160.6 μWh/cm^2, 0.5 mW/cm^2	[67]
Cl-PEDOT	$FeCl_3$	1 mol/L H_2SO_4	−0.2~0.8	480 F/g at 2 A/g	38% (100 A/g)	95% (10,000 cycles)	6.19 Wh/kg, 0.25 kW/kg	[79]
C_{24}-Br-GBr	Br_2 liquids	1 mol/L KCl	−0.2~0.5	258 F/g at 1 A/g	92% (10 A/g)	90% (20,000 cycles)	N/A	[89]
SubPc-Br/ $NiMoO_4$	BBr_3	6 mol/L KOH	0~0.35	1292 F/g at 1 mV/s	22% (100 mV/s)	80% (1000 cycles)	N/A	[90]
I-rGO/ OCY	Iodine steam	6 mol/L KOH	−1~0	1.7 mF/cm at 5 mV/s	12% (300 mV/s)	88% (5000 cycles)	0.1126 μWh/cm, 5 μW/cm	[92]
I-PCs	I_2	1 mol/L H_2SO_4	−0.2~0.8	1216 F/g at 2 A/g	13% (20 A/g)	110% (10,000 cycles)	65.4 Wh/kg, 787.3 W/kg	[93]
IrGO/ rGO	HI (55%)	PVA/H_2SO_4	0~0.8	12.4 mF/cm^2 at 0.01 mA/cm^2	68% (20 mA/cm^2)	89% (5000 cycles)	1.09 μWh/cm^2, 3.99 μW/cm^2	[95]
$Bi_7O_9I_3$	KI	2 mol/L KOH	−1~0	347 F/g at 1 A/g	24% (5 A/g)	66% (5000 cycles)	N/A	[96]
FG/ Niso24h	GrF	1 mol/L Na_2SO_4	0~0.7	391 F/g at 0.25 A/g	51% (10 A/g)	100% (5000 cycles)	N/A	[106]
HA-K-650-M-Q	NaCl	6 mol/L KOH	−1~0	395 F/g at 1 A/g	78% (10 A/g)	87% (10,000 cycles)	32.28 Wh/kg, 2805 W/kg	[107]
PESAC-Cl	HCl	6 mol/L KOH	−1~0 V	242.5 F/g at 1 A/g	85% (5 A/g)	89% (6000 cycles)	21.5 Wh/kg, 385.1 W/kg	[108]

Note: PC: porous carbons; FG: fluorographene; Niso: 5-aminoisophthalic acid; HA-K: potassium humate sample calcined at 650 °C and quenched at 200 °C; PES: poly(ether sulfone); AC: activated carbon.

Table 3
The relationship between hydrophilicity and stability of halogen functionalized electrode materials in aqueous system.

Electrode material	Hydrophilicity	Electrolyte	Cycling stability	Ref.
I-rGO/OCY	Improved	KOH-PVA	88% (5000 cycles)	[92]
FG/Niso24h	Improved	1 mol/L Na_2SO_4	100% (5000 cycles)	[106]
HA-K-650-M-Q	Improved	6 mol/L KOH	87% (10,000 cycles)	[107]
PESAC-Br	Improved	6 mol/L KOH	84.6% (6000 cycles)	[108]

Table 4
The electrochemical performance of different types of electrode materials.

Electrode material	Agent	Cost	Fabrication process	Safety	Remark	Ref.
FGA	40% HF	cheap	easy	caution	High conductivity	[41]
NFHPC	NH_4F/HF	cheap	easy	caution	High graphitization and electric conductivity	[44]
Cl-RGOFs	HCl	cheap	easy	caution	Improved electrical conductivity, high flexibility and practicality	[67]
Cl-PEDOT	$FeCl_3$	cheap	easy	safe	Binder/carbon additive-free	[79]
C_{24}-Br_GBr	Br_2 liquids	hard to buy	complex	caution	High conductivity, glove box	[89]
SubPc-Br/$NiMoO_4$	BBr_3	expensive	easy	caution	Enhanced charge transfer characteristics	[90]
I-rGO/OCY	Iodine steam	cheap	complex	caution	Enhanced electrical conductivity, good hydrophilicity	[92]
I-PCs	I_2	cheap	complex	caution	High specific surface area	[93]

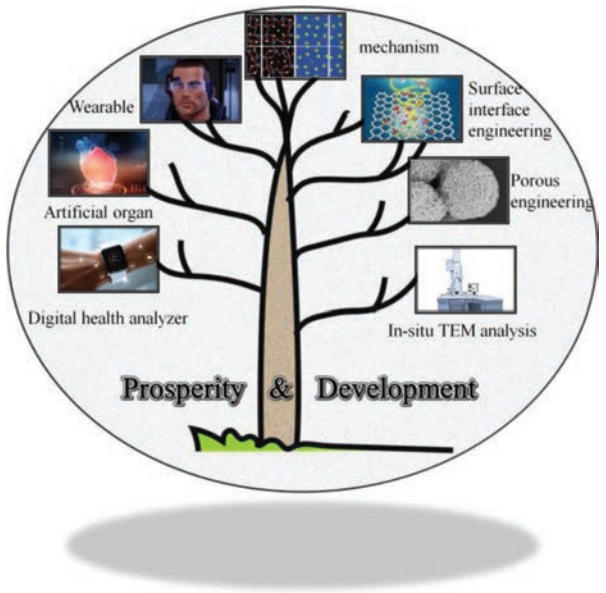

Fig. 10. Prospective of halogen-based functionalized electrode materials for high-performance SCs.

geometric properties of pristine materials (including charge transfer, energy band gap, Gibbs free energy, electron spin density, localized electronic state, and topological defect) can be drastically adjusted in the presence of halogen elements. In addition, the systematical "structure-property" relationship for energy-related SC applications has been comprehensively discussed in this review.

As shown in Table 4, the halogen-based functionalized engineering has shown vast advantages in many aspects. Low cost of raw materials and simple fabrication both make it feasible to achieve the halogen modification. Furthermore, the surface wettability and bulk conductivity can be effectively ameliorated after the introduction of halogen elements. However, a large number of halogenated substances, such as HF, Br_2, will cause huge burdens on the environment and harm to the human body, so this strategy is limited to the preparation scale of laboratories. Although the capacitance can be improved, the cyclic stability of halogen functional groups is being tested. How to balance the specific capacitance and cycling life is also an important research direction in the future.

Although substantial efforts have been performed on halogen-based decorating the electrode materials of SCs towards huge potential, momentous challenges still exist to hinder their basic scientific research and large-scale commercial promotion. Comprehensive electrochemical performance breakthrough rather than individual or certain parameter must be the main focus of future analysis. Based on the analysis of this review, there are several critical issues that should be resolved in the future (Fig. 10).

(1) Detailed discussion on energy storage mechanism. The disclosed effect of diverse halogen doping sites on the final electronic property plays a valuable guidance to the precise structure tailor and targeted synthesis of electrode materials. For example, F-based doping carbon materials may exhibit disparate F sites (armchair-F, bulk-F and zigzag-F) that will result in the confusion to explicit the genuine active configurations for the performance contribution. Currently, the underlying electrochemical mechanism also should not be put aside while the performance improvement is studied, especially for some complexed co-doing or multi-doping cases. Thus, theoretical modeling and calculation of the interface engineering, dynamic evolution of morphology and phase, as well as application-related functional mechanisms are essential for detailed understanding of halogen-based functionalized chemistry in the modification of various metal/nonmental materials. Density of state calculations can accurately present the general state distribution to predict the bandgap structure, which will provide insight into the electrical conductivity and charge storage performance of halogen-based electrode materials. Thus, relevant supported theoretical simulations are supposed to be emerging research technologies to unveil distinct roles of modified halogen species for the enhanced electrochemical performance.

(2) In-depth research on the surface/interface engineering. Surfaces and interfaces are crucial in the fabrication and performance improvement of nano-energy storage materials/devices. Surface/interface engineering can boost superior physicochemical properties and effective synergistic effects for halogen-based functionalized electrode materials, giving knowledge of the novel strategies to improve energy storage activities. Therefore, we should further integrate more active materials through suitable physical and chemical treatment (hydrogen bonding, van der Waals interaction and covalent bonding) for the direct exploitation or modification of the electrode surface chemistry. More alternative approaches should be drawn from the successful reports of other related materials. For electrode materials in SCs, the halogen doping or modification is mainly involved in carbon materials while there are relatively few reports on the field of pseudocapacitive materials. Further innovation in synthetic methods to explore a wider range of material applications and related interface science issues is imperative. Halogen-based functionalized surface/interface engineering methodologies are thus anticipated to endow the active species with adjustable micro-nano structure, tailorable inner accessibility, excellent chemical stability as well as extraordinary capacitance characteristics.

(3) Meticulous analysis on the pore engineering. The pore size structure and porosity of nanomaterials lay great effect on their intrinsic properties. Furthermore, it is desirable for the doping or modification of halogen elements to precisely ad-

just the pore size from the atom to nanometer scale, which highly depends on the processing conditions. We should develop halogen-based hierarchical pore structures for the unobstructed electrode-electrolyte interface and shortened electrolyte ions diffusion length. Meanwhile, we need to design as many methods as possible to control porous networks and avoid structural collapse during the whole long-cycling period. Additionally, the reactive sites may change strikingly and even some materials will undergo a thorough structural reconstruction in the real electrochemical process, which manifest the necessity of *in situ* monitoring. Hence, it is imperative to develop advanced analysis technologies, like *in situ* and/or operando characterization (XRD, XPS, TEM, NMR and synchrotron radiation), in order to deeply gain an accurate identification of atomic-scale correlations and in turn to optimize the material envisage strategies not in terms of trial-and-error approaches [109]. For example, *in-situ* XRD cell is often used to track the phase transition and structural changes of materials within electrodes in real space and time by connecting X-ray diffractometer and electrochemical testing system [110]. Recent developments of advanced TEM technologies also enable *in situ* characterization of dynamically reversible transformation of electrode materials under operational conditions, providing powerful support for visualization during charging and discharging process.

(4) Specification of performance evaluation criteria. Complementally, a set of unified standards are urgently required to be formulated responsible for the electrochemical performance evaluation in the eventual application. For instance, the weight capacitance, areal capacitance and volume capacitance should be taken into account simultaneously, which are significative to the balance between packing density and resistance in devices. Meanwhile, the cycling stability measurement is mentioned in almost every reported literature, yet which is still far from the commercial requirement (over 1,000,000 cycles). Besides, it is applicable to take the long cycling charge-discharge test at the high current density rather than the low current density for reflecting the stability more accurately [111].

(5) Compatibility with flexible devices. The forthcoming intelligent electronic era requires the development of advanced flexible devices with miniaturization, lightweight, shape memory, high mechanical strength and superior energy storage performance. The strong entangled interconnection between electrodes and electrolytes/separators should be preserved during the whole halogen-based functionalization process. Moreover, high conductivity and mechanical robustness also need to be achieved by integrated with other flexible active material (nanocellulose) while packaging to maximize the contribution of each component.

In a nutshell, the rational introduction of halogen species into electrode active materials will trigger the synergistic effects which can retain the best advantages of related components and endue new chemical environment, thus enhancing the electrochemical performance. However, there is still a long way to address some key issues on urgent basis. The integration of experimental and theoretical researches is anticipated to unveil the general principle for controllably tuning the halogen-based doping strategy, which will contribute to the overall development of SC electrodes and can also provide referential guidance for other heteroatom-based doping strategies. In short, we are looking forward to that this research progress review can offer meaningful insights into the reasonable design of halogen-based functionalized chemistry for high performance SC applications, thereby attracting more meaningful research interests.

Declaration of competing interest

The authors declare no conflict of interest.

Acknowledgments

This work was financially supported by the Major Program of Zhejiang Provincial Natural Science Foundation of China (No. LD22B030002), Zhejiang Provincial Ten Thousand Talent Program and the Independent Designing Scientific Research Project of Zhejiang Normal University (No. 2020ZS03).

References

[1] C. Choi, D.S. Ashby, D.M. Butts, et al., Nat. Rev. Mater. 5 (2020) 5–19.
[2] Y. Shao, M.F. El-Kady, J. Sun, et al., Chem. Rev. 118 (2018) 9233–9280.
[3] J. Liu, J. Wang, C. Xu, et al., Adv. Sci. 5 (2018) 1700322.
[4] F. Wang, X. Wu, X. Yuan, et al., Chem. Soc. Rev. 46 (2017) 6816–6854.
[5] T.S. Mathis, N. Kurra, X. Wang, et al., Adv. Energy Mater. 9 (2019) 1902007.
[6] W. Zuo, R. Li, C. Zhou, et al., Adv. Sci. 4 (2017) 1600539.
[7] C. Li, J. Balamurugan, N.H. Kim, J.H. Lee, Adv. Energy Mater. 8 (2018) 1702014.
[8] J. Balamurugan, C. Li, V. Aravindan, N.H. Kim, J.H. Lee, Adv. Funct. Mater. 28 (2018) 1803287.
[9] Z. Pan, M. Liu, J. Yang, et al., Adv. Funct. Mater. 27 (2017) 1701122.
[10] G. Xiong, P. He, D. Wang, et al., Adv. Funct. Mater. 26 (2016) 5460–5470.
[11] G. Sun, X. Zhang, R. Lin, et al., Angew. Chem. Int. Ed. 54 (2015) 4651–4656.
[12] N. Sulaiman, M.A. Hannan, A. Mohamed, et al., Appl. Energy 228 (2018) 2061–2079.
[13] L. Kouchachvili, W. Yaïci, E. Entchev, J. Power Sources 374 (2018) 237–248.
[14] M.K. Döşoğlu, O. Özkaraca, U. Güvenç, Electr. Eng. 101 (2019) 1119–1132.
[15] L. Kong, J. Yu, G. Cai, Int. J. Hydrog. Energy 44 (2019) 25129–25144.
[16] Y.S. Perdana, S.M. Muyeen, A. Al-Durra, H.K. Morales-Paredes, M.G. Simões, IEEE Trans. Sustain. Energy 10 (2019) 1370–1379.
[17] M.S. Masaki, L. Zhang, X. Xia, Appl. Energy 242 (2019) 393–402.
[18] W. Lu, J. Shen, P. Zhang, et al., Angew. Chem. Int. Ed. 58 (2019) 15441–15447.
[19] M. Yu, X. Cheng, Y. Zeng, et al., Angew. Chem. Int. Ed. 55 (2016) 6762–6766.
[20] Z. Yuan, H. Wang, J. Shen, et al., J. Mater. Chem. A 8 (2020) 22163–22174.
[21] L. Feng, K. Wang, X. Zhang, et al., Adv. Funct. Mater. 28 (2018) 1704463.
[22] W. Ye, H. Wang, J. Ning, Y. Zhong, Y. Hu, J. Energy Chem. 57 (2021) 219–232.
[23] H. Wang, Y. Yang, Q. Li, et al., Sci. China Mater. 64 (2021) 840–851.
[24] N. Chen, X. Huang, L. Qu, Phys. Chem. Chem. Phys. 17 (2015) 32077–32098.
[25] T. Wang, X. Zang, X. Wang, et al., Energy Storage Mater. 30 (2020) 367–384.
[26] X. Zhang, X. Liu, Y. Zeng, Y. Tong, X. Lu, Small Methods 4 (2020) 1900823.
[27] S. Ghosh, S. Barg, S.M. Jeong, K. Ostrikov, Adv. Energy Mater. 10 (2020) 2001239.
[28] F. Wang, L. Chen, H. Li, et al., Chin. Chem. Lett. 31 (2020) 1986–1990.
[29] C. Li, X. Zhang, K. Wang, et al., J. Energy Chem. 54 (2021) 352–367.
[30] C. Li, X. Zhang, Z. Lv, et al., Chem. Eng. J. 414 (2021) 128781.
[31] Y. Gu, L. Miao, Y. Yin, et al., Chin. Chem. Lett. 32 (2021) 1491–1496.
[32] M. Zhang, W. Wang, X. Liang, et al., Chin. Chem. Lett. 32 (2021) 2217–2221.
[33] H. Wang, W. Ye, Y. Yang, Y. Zhong, Y. Hu, Nano Energy 85 (2021) 105942.
[34] Y. Yang, D. Chen, H. Wang, et al., Chem. Eng. J. 431 (2022) 133250.
[35] Q. Abbas, R. Raza, I. Shabbir, A.G. Olabi, J. Sci. Adv. Mater. Dev. 4 (2019) 341–352.
[36] X. Zhao, Z. Zhao-Karger, M. Fichtner, X. Shen, Angew. Chem. Int. Ed. 59 (2020) 5902–5949.
[37] P. Jadhav, G.M. Joshi, J. Polym. Res. 28 (2021) 73.
[38] M. Gu, B.S. Kim, Acc. Chem. Res. 54 (2021) 57–69.
[39] Y. Gao, Q. Wang, G.Z. Ji, A.M. Li, J.M. Niu, RSC Adv. 11 (2021) 5361–5383.
[40] N.P.D. Ngidi, M.A. Ollengo, V.O. Nyamori, Int. J. Energy Res. 43 (2019) 1702–1734.
[41] T. Jin, J. Chen, C. Wang, Y. Qian, L. Lu, J. Mater. Sci. 55 (2020) 12103–12113.
[42] S. Saha, P. Samanta, N.C. Murmu, et al., Chem. Eng. J. 339 (2018) 334–345.
[43] T. Zhu, S. Liu, K. Wan, et al., ACS Appl. Energy Mater. 3 (2020) 4949–4957.
[44] Y. Zhao, C. Huang, Y. He, et al., J. Power Sources 456 (2020) 228023.
[45] Y. Geng, Y. Song, M. Zhong, et al., Mater. Lett. 64 (2010) 2673–2675.
[46] R.R. Nair, W. Ren, R. Jalil, et al., Small 6 (2010) 2877–2884.
[47] M.H. Kim, J.H. Yang, Y.M. Kang, et al., Colloids Surf. A: Physicochem. Eng. Asp. 443 (2014) 535–539.
[48] H. An, Y. Li, P. Long, et al., J. Power Sources 312 (2016) 146–155.
[49] E. Jokar, S. Shahrokhian, A. Iraji, E. Asadian, H. Hosseini, J. Energy Storage 17 (2018) 465–473.
[50] C. Sun, Y. Feng, Y. Li, et al., Nanoscale 6 (2014) 2634–2641.
[51] R. Zhang, Z.L. Liu, T.N. Gao, et al., Angew. Chem. Int. Ed. 60 (2021) 24299–24305.
[52] Y. Gao, C. Zhi, P. Cui, et al., Chem. Eng. J. 400 (2020) 125967.
[53] D. Zhang, X. Han, X. Kong, F. Zhang, X. Lei, Nano-Micro Lett. 12 (2020) 107.
[54] M. Hu, Z. Li, T. Hu, et al., ACS Nano 10 (2016) 11344–11350.
[55] M.R. Lukatskaya, S.M. Bak, X. Yu, et al., Adv. Energy Mater. 5 (2015) 1500589.

[56] S. Kumar, D. Kang, H. Hong, et al., RSC Adv. 10 (2020) 41837–41845.
[57] J. Chen, H. Chen, M. Chen, et al., Chem. Eng. J. 428 (2022) 131380.
[58] C. Lu, L. Yang, B. Yan, et al., Adv. Funct. Mater. 30 (2020) 2000852.
[59] D. Liu, Q. Li, H. Zhao, J. Mater. Chem. A 6 (2018) 11471–11478.
[60] T. Aytug, M.S. Rager, W. Higgins, et al., ACS Appl. Mater. Interfaces 10 (2018) 11008–11017.
[61] L. Jiang, L. Sheng, C. Long, Z. Fan, Nano Energy 11 (2015) 471–480.
[62] Z. Song, Y. Fan, Z. Sun, et al., J. Mater. Chem. A 5 (2017) 20797–20807.
[63] Y. Xu, C.Y. Chen, Z. Zhao, et al., Nano Lett. 15 (2015) 4605–4610.
[64] G.G. Jang, B. Song, L. Li, et al., Nano Energy 32 (2017) 88–95.
[65] Z. Pan, H. Zhi, Y. Qiu, et al., Nano Energy 46 (2018) 266–276.
[66] Z. Song, W. Li, Y. Bao, et al., Carbon 136 (2018) 46–53.
[67] H. Jiang, X. Ye, Y. Zhu, et al., ACS Sustain. Chem. Eng. 7 (2019) 18844–18853.
[68] N. Mahmood, M. Tahir, A. Mahmood, et al., Nano Energy 11 (2015) 267–276.
[69] Y. Zhao, S. Liu, B. Zhang, et al., Nanoscale Res. Lett. 13 (2018) 415.
[70] G.A. Snook, P. Kao, A.S. Best, J. Power Sources 196 (2011) 1–12.
[71] C. Xia, W. Chen, X. Wang, et al., Adv. Energy Mater. 5 (2015) 1401805.
[72] M. Rajesh, C.J. Raj, B.C. Kim, et al., Electrochim. Acta 220 (2016) 373–383.
[73] W. Qingshuo, M. Masakazu, K. Kazuhiro, N. Yasuhisa, I. Takao, Materials 8 (2015) 732–750.
[74] B. Xu, S.A. Gopalan, A.I. Gopalan, et al., Sci. Rep. 7 (2017) 46779.
[75] H. Shi, C. Liu, Q. Jiang, J. Xu, Adv. Electron. Mater. 1 (2015) 1500017.
[76] B. Cho, K. Park, J. Baek, et al., Nano Lett. 14 (2014) 3321–3327.
[77] N. Massonnet, A. Carella, A. de Geyer, J. Faure-Vincent, J.P. Simonato, Chem. Sci. 6 (2015) 412–417.
[78] S.G. Im, K.K. Gleason, Macromolecules 40 (2007) 6552–6556.
[79] M. Rajesh, R. Manikandan, B.C. Kim, et al., Electrochim. Acta 354 (2020) 136669.
[80] W. Liu, M. Ulaganathan, I. Abdelwahab, et al., ACS Nano 12 (2018) 852–860.
[81] P. Katti, K.V. Kundan, S. Kumar, S. Bose, Polymer 122 (2017) 184–193.
[82] V. Georgakilas, M. Otyepka, A.B. Bourlinos, et al., Chem. Rev. 112 (2012) 6156–6214.
[83] A. Keerthi, B. Radha, D. Rizzo, et al., J. Am. Chem. Soc. 139 (2017) 16454–16457.
[84] G. Bottari, M.Á. Herranz, L. Wibmer, et al., Chem. Soc. Rev. 46 (2017) 4464–4500.
[85] H. Au, N. Rubio, M.S.P. Shaffer, Chem. Sci. 9 (2018) 209–217.
[86] Z. Liu, H. Zhou, Z. Huang, et al., J. Mater. Chem. A 1 (2013) 3454–3462.
[87] Y. Liang, D. Wu, X. Feng, K. Müllen, Adv. Mater. 21 (2009) 1679–1683.
[88] R. Khan, R. Nakagawa, B. Campeon, Y. Nishina, ACS Appl. Mater. Interfaces 12 (2020) 12736–12742.
[89] C. Hu, Q. Yue, F. Zhao, et al., CCS Chem. 2 (2020) 1872–1883.
[90] B.B. Zhang, H. Hao, F.Y. Zhang, et al., J. Appl. Electrochem. 50 (2020) 1007–1018.
[91] Z. Xiao, Z. Yang, L. Zhang, H. Pan, R. Wang, ACS Nano 11 (2017) 8488–8498.
[92] P. Zhao, X. Ye, Y. Zhu, et al., J. Power Sources 442 (2019) 227188.
[93] X. Luo, Y. Wang, Z. Shen, et al., J. Colloid Interface Sci. 599 (2021) 351–359.
[94] B. Yan, S. Matsushita, S. Suzuki, et al., Carbohydr. Polym. 196 (2018) 332–338.
[95] J. Yang, J. Zhang, X. Li, et al., Nano Energy 53 (2018) 916–925.
[96] P. Wu, L. Feng, Y. Liang, et al., J. Mater. Sci: Mater. Electron. 31 (2020) 5385–5401.
[97] Y. Gao, J. Zhang, X. Luo, et al., Nano Energy 72 (2020) 104666.
[98] D. Liu, K. Ni, J. Ye, et al., Adv. Mater. 30 (2018) e1802104.
[99] R. Vinodh, P.J.S. Rana, C.V.V.M. Gopi, et al., Polym. Int. 68 (2019) 929–935.
[100] Z. Liu, Y. Huang, Y. Huang, et al., Chem. Soc. Rev. 49 (2020) 180–232.
[101] M.H. Alfaruqi, V. Mathew, J. Gim, et al., Chem. Mater. 27 (2015) 3609–3620.
[102] B. Tang, G. Fang, J. Zhou, et al., Nano Energy 51 (2018) 579–587.
[103] J. Cheng, Y.H. Wen, G.P. Cao, Y.S. Yang, J. Power Sources 196 (2011) 1589–1592.
[104] X. Li, Y. Tang, J. Zhu, et al., Small 16 (2020) 2001935.
[105] Q.Q. Qiu, S.S. Yuan, J. Bao, et al., J. Energy Chem. 61 (2021) 574–581.
[106] E.C. Vermisoglou, P. Jakubec, A. Bakandritsos, et al., Chem. Mater. 31 (2019) 4698–4709.
[107] T. Liu, Y. Lan, Q. Zhu, et al., Chem. Eng. J. 421 (2021) 129993.
[108] W. Zhang, L. Zhao, H. Li, P. Manasa, F. Ran, J. Power Sources 491 (2021) 229612.
[109] D.B. Kong, Y. Gao, Z.C. Xiao, et al., Adv. Mater. 31 (2019) 1804973.
[110] M. Xia, T. Liu, N. Peng, et al., Small Methods 3 (2019) 1900119.
[111] Y. Gogotsi, R.M. Penner, ACS Nano 12 (2018) 2081–2083.